Review

Towards a Model for Albitite-Type Uranium

Andy Wilde

Geology and Mining Department, Paladin Energy Ltd., Subiaco, Western Australia 6008, Australia;
E-Mail: andy.wilde@paladinenergy.com.au; Tel.: +61-(8)-9381-4366; Fax: +61-(8)-9381-4978

Abstract: Albitite-type uranium deposits are widely distributed, usually of low grade (<1% U_3O_8), but are often large and collectively contain over 1 million tonnes of U_3O_8. Uranium is hosted in a wide range of metamorphic lithologies, whose only common characteristic is that they have been extensively mylonitised. Ore minerals are disseminated and rarely in megascopic veins, within and adjacent to albitised mylonites. Grain size is uniformly fine, generally less than 50 microns. Scanning electron microscopy reveals that spatial association between uranium and various Ti-bearing phases is common. Gangue minerals include albite, carbonates (calcite and dolomite), and sodic pyroxene and amphibole. The ore rarely contains economic metals apart from uranium, phosphorous at Itataia being an exception. There is widespread evidence of hydrothermal zirconium mobility and hydrothermal zircon and other Zr phases are frequent and in some cases abundant gangue minerals. Positive correlations are noted between uranium and various high field strength elements. The group remains poorly described and understood, but a link to iron-oxide copper-gold (IOCG) deposits and/or carbonatite and/or alkaline magmatism is plausible.

Keywords: uranium; albitite; low-grade; Proterozoic; high field strength elements; mylonite

1. Introduction

Albitite-type uranium deposits (also known as metasomatite- or Na-metasomatite-type deposits) are widely distributed and collectively contain as much uranium as the better known unconformity-type deposits, although at grades which are typically an order of magnitude or more lower. Mines exploiting albitite-type deposits currently operate in the Kirovograd-Krivoi Rog district of the Ukraine and at Lagoa Real in Brazil and have operated historically in the Beaverlodge district of Canada. It is thus

clear that the deposit class is economically significant. Exploration and development of these deposits, however, is hampered by relatively sparse literature and albitite-type uranium deposits are among the least well understood uranium deposits. In this paper I have attempted to review key literature and to present a largely descriptive model, but emphasise that more research is needed in order to better understand the genesis of this deposit group and to develop predictive exploration paradigms.

Figure 1 illustrates the distribution of major albitite-type uranium deposits. Some of the main districts and deposits are listed in Table 1. Probably the type area for this type of deposit is the Kirovograd-Krivoi Rog district of the Ukraine. Mines in this area have been in production since the nineteen sixties and overall uranium endowment probably exceeds 250,000 t U. The Novokonstaninovsk deposit alone contains over 93,600 t U at 0.14% U. Other major deposits and districts include Itataia (Santa Quiteria) and Lagoa Real in Brazil, the Central Mineral Belt of Labrador, Canada, the Mount Isa district in Queensland, Australia, and the Beaverlodge district of Saskatchewan, Canada. Sparse data suggest that the massive Elkon district (>300 million tonnes U_3O_8) in Russia may also be of albitite-type. Thus the total contained resource of the deposit group is probably in excess of 1 million tonnes.

Figure 1. Location of albitite-type (and related) uranium deposits.

Table 1. Some details for some major albitite-type uranium provinces. Note that many deposits were probably deposited at *ca.* 1.8 Ga, perhaps synchronous with the volcanic host-rocks to the Central Mineral Belt and Mount Isa district.

District or Deposit	Country	Endowment (kt U_3O_8)	Host-Rock	Host-Rock Age	Ore Age (Ga)	Main Deposits
Kirovo-Grad	Ukraine	>250	Gneiss, granite, iron-rich rocks	Archaean–Orosirian	1.90–1.70	Novaya, Severinskoye Novokonstantinovskoye
Itataia	Brazil	142	Mylonitic marble, calc-silicate rock and gneiss	Orosirian–Stratherian	No Data	Itataia

Table 1. *Cont.*

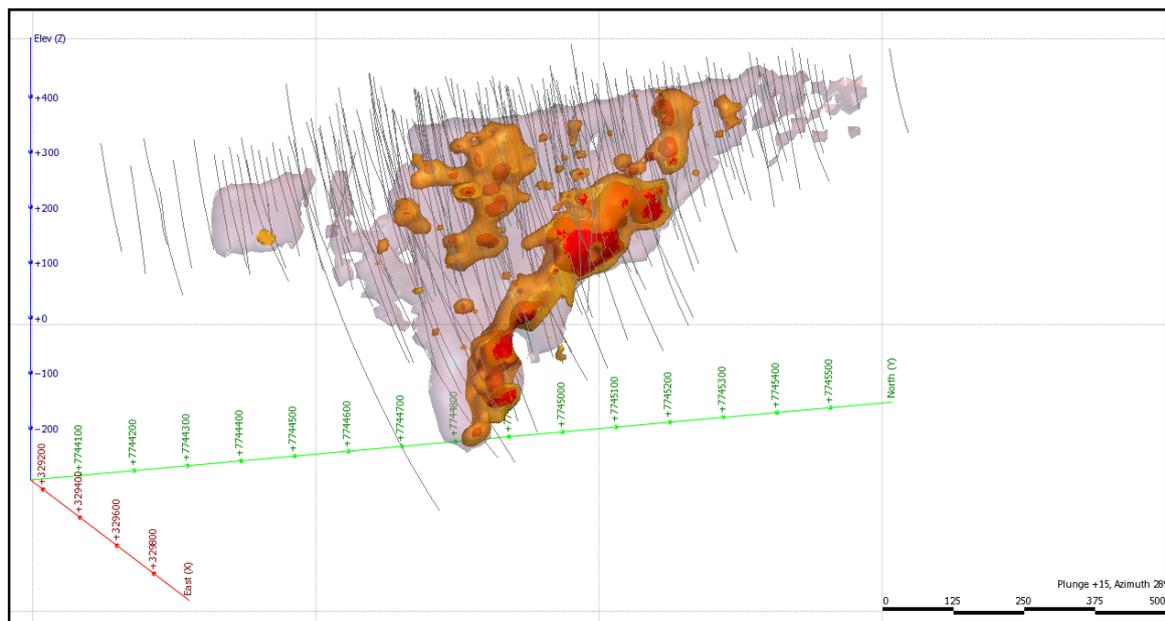| District or Deposit	Country	Endowment (kt U$_3$O$_8$)	Host-Rock	Host-Rock Age	Ore Age (Ga)	Main Deposits
Lagoa Real	Brazil	100	Mylonitised gneiss (large scale ductile shear zone)	Orosirian	1.87 ± 0.07 0.6 ± 0.2	Cachoeira, Rabicha
Central Mineral Belt	Canada	74	Mylonitised meta-rhyolite, meta-volcaniclastic rocks and metasediments	Orosirian	1.83 ± 0.03	Michelin, Jacque's Lake, Kitts, Moran Lake
Mount Isa	Australia	57	Mylonitised meta-basalt and meta-siltstone	Orosirian	1.56–1.51	Valhalla, Odin, Skal, Bikini
Beaver-Lodge	Canada	30	Mylonitised and/or cataclased granitic gneiss and amphibolite	Archaean to Orosirian	1.86–1.78 ± 0.02	Fay, Ace, Verna, Gunnar

2. Host Rocks & Structural Setting

Albitite-type uranium deposits and districts are exclusively located in Proterozoic metamorphic terranes, particularly those dominated by Orosirian rocks (1.8 Ga to 2.05 Ga). Almost all descriptions associate the deposits with zones of mylonitisation and/or cataclasis. Deposits in the Kirovograd-Krivoi Rog district, for example, are localised adjacent to deep-penetrating faults that extend over 100 km at surface and are marked by a combination of pegmatite intrusion, cataclasis and mylonitisation [1,2]. The Beaverlodge district is another example where deposits are hosted within a major fault zone, the St Louis Fault, defined by wide zones (>1 km) of mylonitisation and also by relatively late brittle structures. In the Mount Isa district, deposits are widely scattered, but the largest deposits (Valhalla, Odin, Skal and Bikini) are within kilometers of the regionally extensive Mt Isa fault zone, which is marked by prominent magnetic and gravity gradients, and which can be recognised in potential field data at depths of over 5 km. At surface the manifestation of this major fault zone is limited to sporadic outcrops due to weathering and transported cover. Uranium at Lagoa Real is finely disseminated in discontinuous tabular albitites developed along shear zones [3,4]. Mineralization at Aricheng (Guyana) occurs in two sub-parallel, east-west trending fault breccia zones in albitized granodiorite and monzonite of the Kurupung Batholith [5,6].

Structural controls on deposit location deserve more research. It is apparent that one crucial factor is the presence of major zones of mylonitisation. In those cases where information is available on orebody morphology it can be seen that the ore zones typically form steeply plunging and flattened linear bodies within the mylonite zones. Uranium at Valhalla (Queensland) and Michelin (Labrador) occurs as remarkably similar, south-plunging, steeply plunging shoots within a planar north-south to north-east striking zone of albitisation (Figure 2). At Valhalla this structurally-controlled uranium

mineralisation is hosted in greenschist facies metabasalt and interbedded meta-siltstone and a major control on ore shoot disposition appears to be the intersection of lithological contacts between meta-basalt and meta-siltstone and the discordant albitite (mylonite) zone. Alteration intensity in the deposits of the Kirovograd region has been related to the degree of interbedding, with alteration only weakly developed in homogeneous rocktypes [1].

Figure 2. Morphology of the Valhalla orebody. Pink–albitite; Yellow–low grade ore; Red–high grade ore.
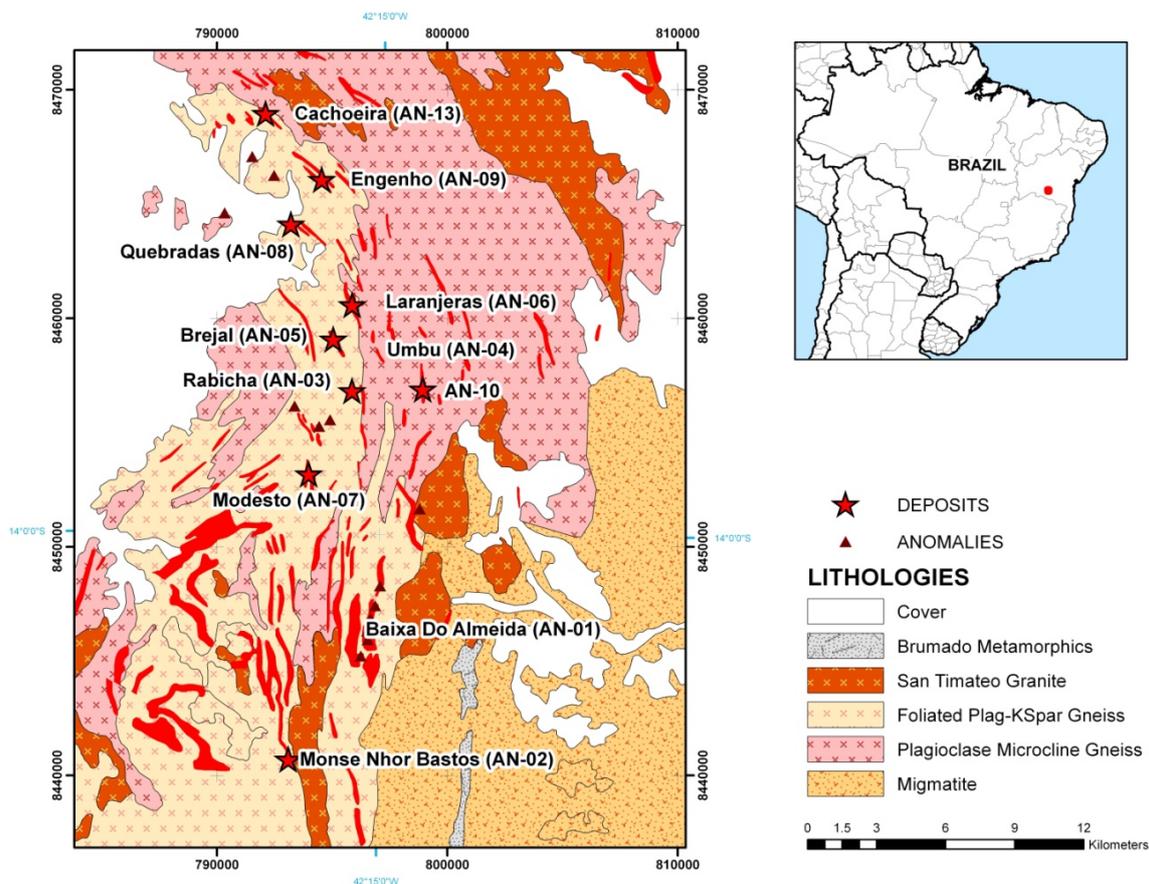

A wide range of lithologies contain economic mineralization, ranging from gneissic granite to iron-rich meta-sediments, meta-basalt and meta-rhyolite. The group shows lack of preference for a specific rock-type and there appears to be little in common either chemically or mineralogically between the various host-rocks. Twenty deposits of the Kirovograd region are hosted in albitised granites and granitic gneiss complexes [7]. At the Novaya mine, uranium is associated with albitite developed in magnetite amphibole schist, alkaline amphibole rocks and mica schist [8]. It is not clear, however, the degree to which these rocks have been modified by hydrothermal alteration processes. More than thirty U and P deposits and prospects occur within albitised granite gneisses, amphibolite gneisses, marbles and migmatitic granite of the Early Proterozoic Santa Quiteria Massif in Brazil [9]. The giant Itataia (or Santa Quiteria) U-P deposit is hosted by Early Proterozoic marble (containing graphite, phlogopite, diopside and tremolite) and sillimanite-garnet-biotite gneiss [10]. Deposits at Lagoa Real in are also hosted in granitoid gneiss [3]. The Aricheng deposit is hosted in the Early Proterozoic Kurupung batholith which consists of monzogabbro, monzonite, monzogranite and peraluminous leucogranites [5].

A number of deposits are hosted in metamorphosed volcanic rocks. Michelin and Jacque's Lake of the Central Mineral Belt of Labrador are hosted within rhyolitic to intermediate meta-volcanic and volcaniclastic rocks. The Valhalla, Odin, Bikini and Skal deposits of the Mount Isa uranium district (Queensland, Australia) are hosted within meta-basalt and interbedded meta-siltstones of the Eastern Creek Volcanics.

3. Albitites and Uranium

A defining characteristic of these deposits is the almost ubiquitous association of economic uranium with albitite. This implies a fundamental link between uranium emplacement and the processes of albitisation. Unfortunately, there is a paucity of data on the regional distribution of albitites within the various mineralised terranes, the exception being Lagoa Real. Figure 3 demonstrates that albitites of the Lagoa Real district are far more extensive than the associated uranium mineralization. At Mount Isa, albitites are similarly extensive, and a spatial and temporal association has been noted not only between albitite and uranium but also between albitite and copper and gold of IOCG type [11]. Most albitites in the Mount Isa region appear to be devoid of either uranium or copper and gold. Kalyaev [12] noted of the Kirovograd deposits that "albitisation is necessary for uranium mineralization but is not sufficient by itself: other conditions are also necessary". These "other conditions" remain poorly defined.

Figure 3. Relationship of uranium deposits to regional albititisation, Lagoa Real district of Brazil. Modified after [3]. Distribution of albitites shown in red.
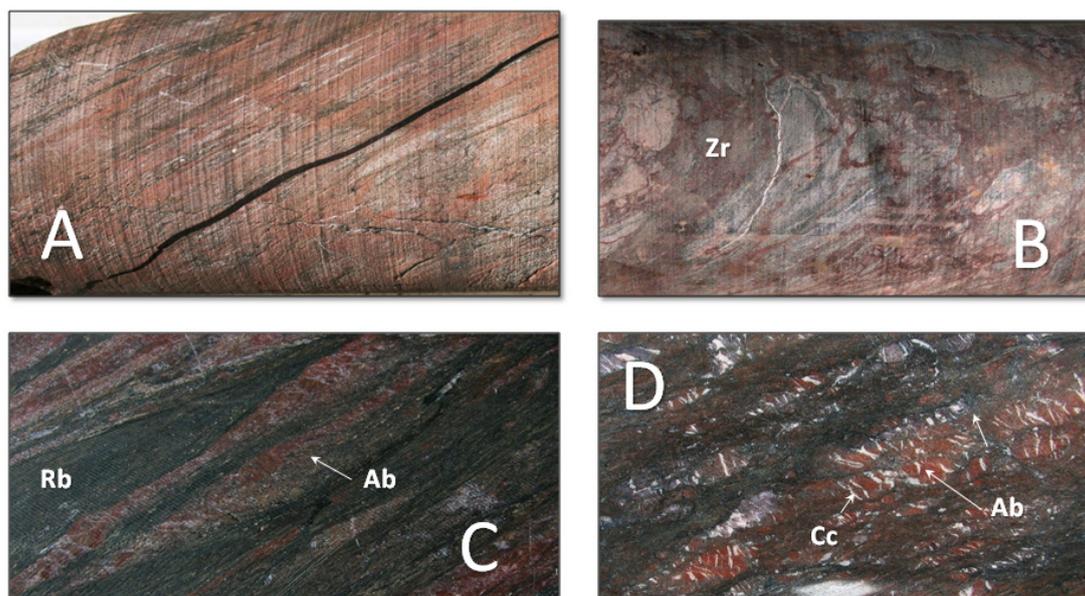

Albitites are often readily identifiable in the field because of various shades of red and pink, often contrasting markedly with the host-rocks. In some works albitised granitoid rocks are referred to as "episyenite" [9]. Red or pink colouration is due to the presence of fine-grained disseminated hematite or hydrothermal apatite. A common feature is vuggy porosity, but this is by no means universal. This porosity can be a reflection of dramatic bulk chemical changes, including almost complete removal of

K and depletion in Si due to quartz and K-feldspar dissolution. For example, vugs resulting from the removal of quartz at Aricheng were filled sequentially by albite, carbonate minerals, chlorite and crypto-crystalline silica [6]. In the Beaverlodge district (Gunnar deposit), however, vuggy texture is considered to be the result of dissolution of carbonate minerals in the near surface environment [13].

Uranium is disseminated in albitite and only rarely forms veins that are visible to the naked eye (Figure 4A). There are some examples, however, such as the Jacque's Lake deposit (Central Mineral Belt) and the Ace-Fay-Verna deposits (Beaverlodge District) in which the bulk of uranium is vein-hosted [13–16]. Breccia textures are common and uranium tends to occupy breccia matrix. Figure 4B shows an example of breccia ore from the Valhalla deposit that is cemented by a matrix of hydrothermal zircon and uranium. Figure 4C,D illustrate textures common in the deposits at Mount Isa. Elongate fragments of albitite are enclosed in a schistose matrix dominated by riebeckite. It would appear that the albitite fragments deformed by fracturing (with subsequent infilling by calcite) whereas the matrix deformed in more ductile fashion.

Uranium can be demonstrated in many (perhaps most) cases to have been introduced after pervasive albitisation of the host-rocks and to be spatially and temporally associated with micro-fracturing or complete brecciation of the albitite [1,2,17–19]. Thus, brecciation appears to be a key factor in generating porosity and permeability in the albitites [1]. Indeed, measurements appear to indicate that albitites are today significantly more porous and permeable than the host rocks [2]. Chemical dissolution has probably contributed also to the generation of abnormal porosity and permeability.

Figure 4. Relationship of uranium deposits to regional albititisation. (**A**) typical mylonite ore; (**B**) hydrothermal breccia ore with zircon-U matrix; (**C**) Early albitite fragments in riebeckite schist with later calcite veins; (**D**) An example similar to (**C**) with more intense carbonate veining. Ab–albite, Zr–zircon, Rb–riebeckite, cc–calcite.
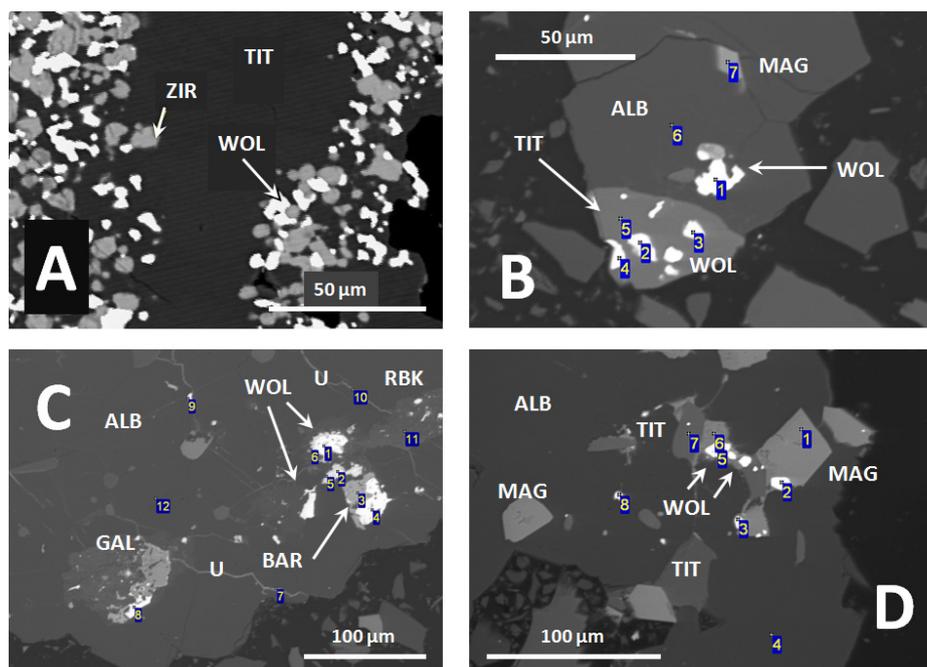

4. The Ores at the Microscopic Scale

The ores have several key microscopic features. One is the fine grain size (typically < 50 microns) of uranium minerals. Scanning electron microscopy is desirable in order to identify ore minerals with

confidence, and in some instances even the spatial resolution of the scanning electron microscope (SEM) is inadequate [19]. Another feature is the wide range of primary uranium minerals, including uraninite, coffinite, wolsendorfite, brannerite, nenadkevite (a uranium silicate possibly equivalent to thorite $(U,Th)SiO_4$), fourmarierite, hawaiite, uraniferous zircon, zircon "gel", as well as uraniferous titanite, rutile, ilmenite and magnetite [1,2,5,6]. A third feature of the ore is the frequent spatial association of U and Ti. A significant portion (5%–10%) of uranium at many of the deposits occurs in U-Ti phases including what is referred to as brannerite (Figure 5). Field emission gun electron probe microanalysis of minerals described as brannerite from Valhalla, Skal and Bikini yield non-stoichiometric analyses and these may be an unnamed mineral [19]. Uranium also frequently occurs as inclusions in titanite, rutile and less commonly ilmenite.

Figure 5. SEM Images of ore from Jacque's Lake showing typical occurrence of uranium as inclusions in titanite (TIT) magnetite and albite (ALB). Andy Wilde unpublished data. (**A**) Intimate association of uranium with zircon as inclusions in titanate; (**B**) Uranium as wolsendorfite inclusions in titanate; (**C**) Uranium as wolsendorfite (WOL) associated with riebeckite (RBK) and barytes (BAR) included in albite; (**D**) Uranium as wolsendorfite inclusions in titanite and magnetite.
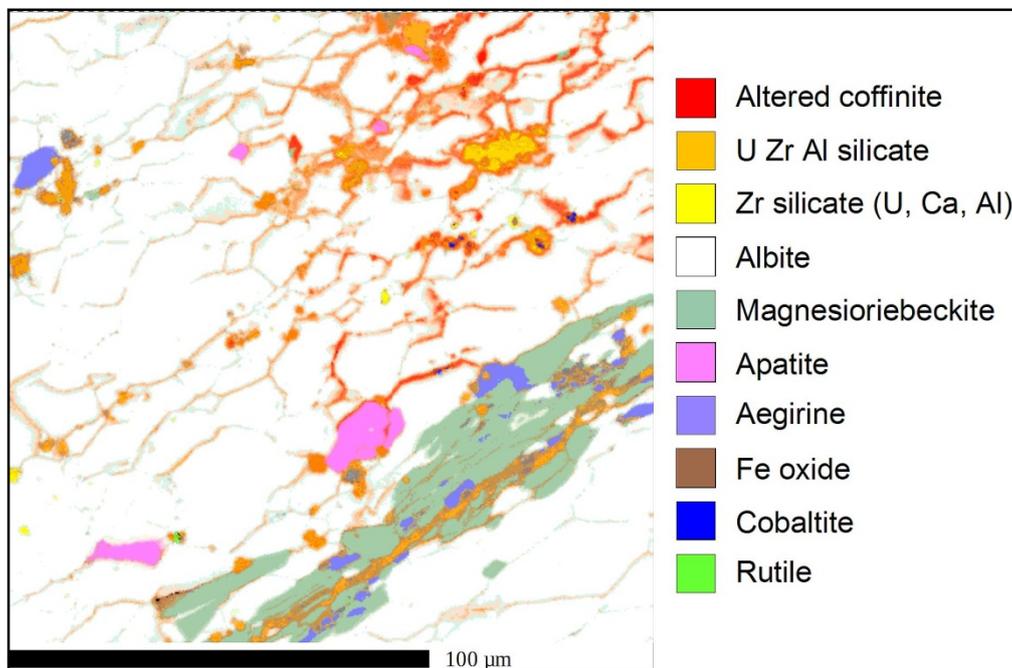

There appears to be two main modes of occurrence of uranium minerals. One is as inclusions in a variety of phases but typically titanite and amphibole (Figure 5), the other is as microveinlets (Figure 6).

Gangue phases include albitic feldspar, quartz, calcite, dolomite, sodic amphibole (riebeckite and magnesio-riebeckite), sodic pyroxene (aegirine), chlorite, biotite, epidote (and/or allanite), magnetite, hematite, titanite, ilmenite, zircon and apatite [1,2,5,6,19]. The Itataia deposit is extremely rich in apatite and apatite is a significant hydrothermal phase in most if not all albitite type uranium deposits. There is consistent evidence of hydrothermal Zr mobility in the deposits. At Aricheng, hydrothermal zircon occurs with albite in vugs and as veins up to 1 cm wide in albitised host rocks [6]. Hydrothermal zircon makes up to 80% of the rock in some parts of the deposit [5]. Massive zircon

cements breccias at the Valhalla deposit (Figure 5B). Sulphide minerals are generally present only in trace quantities.

Figure 6. FEG-SEM Images of ore from Valhalla showing typical occurrence of uranium [19].

Alteration zonation over 1.5 km vertical depth has been documented in the Kirovograd deposits [20]. High temperature phases such as riebeckite and aegirine are common at depth but give way to chlorite and epidote in the upper 700 m. Aegirine increases in abundance relative to riebeckite with depth. At Mount Isa the highest ore tonnages are associated with riebeckite and aegirine dominant alteration, notably at Valhalla and Odin, while other deposits contain much higher chlorite and lesser albitite (Skal and Bikini). A minor portion of the overall uranium resource in the Lagoa Real district is hosted within granoblastic epidosite [3]. The observed hydrothermal alteration zonation has been attributed to falling temperature as hydrothermal fluids moved upwards, coupled with increased pH and lower Na activity [20].

5. Chemical Characteristics of the Ores

Table 2 presents bulk chemical data for several albitite-type uranium deposits. I have distinguished between ore-grade samples and those with less than 500 ppm U. While correlations differ between deposits, there are many consistent positive correlations, particularly with some or all of the high field strength elements (Zr, Nb, Hf, REE, Th, U, Ta). REE concentrations are generally anomalous, but seldom to the point of being considered to be an economic byproduct to uranium. Silver is another element that consistently correlates with uranium.

Table 2. Summary of bulk chemical characteristics of selected albitite-type uranium deposits. (Paladin Energy unpublished data, except Lagoa Real and Itataia [9,21]. Note that analytical suites, methods and detection limits vary between deposits).

Deposit	Sample Population	# Samples	Correlation Coefficients with U >0.50	Correlation Coefficients with U 0.50–0.35	Comments
Lagoa Real	All available samples Major Elements	39	MgO (0.69), CaO (0.52)	TiO$_2$ (0.37), Na$_2$O (0.36)	Suite of 15 minor elements analysed for, including V, Y & Nb. REE not analysed for.
	All available samples Minor Elements	39	**Pb** (0.77), **Nb** (0.85)	Th (0.58), V (0.48), Ni (0.43), **Zr** (0.40)	
Itataia	All available samples Major Elements	86	CO$_2$ (0.78), S (0.73)	Fe$_2$O$_3$ (0.42), P$_2$O$_5$ (0.38), CaO (0.34)	Only U and Zr of minor elements were analysed for and not in all samples.
Valhalla	U > 500 ppm	2425	Be (0.57), Y (0.57), Sr (0.51), Ag (0.51)	**Zr** (0.47), Ce (0.41)	Ga, Hf not analysed. Bi, Nb & Ta consistently BLD.
	All available samples Major Elements	94	No correlation	Na$_2$O (0.44), LOI (0.36)	
	All available samples Minor Elements	12173	**Pb** (0.72), Yb (0.58), **Th** (0.56), **Zr** (0.56)	Dy (0.48), Y (0.38), Sr (0.42), V (0.43), As (0.43)	
Michelin	U > 500 ppm	1464	**Ag** (0.76), **Pb** (0.66), Ga (0.55)	Zr (0.37)	Cs, Hf, Nb, Sn, most REE, Y, Yb analysed in only 214 samples (*i.e.*, about 5% of total samples).
	All available samples Major Elements	214	No correlation	Na$_2$O (0.49), Al$_2$O$_3$ (0.44)	
	All available samples Minor Elements	5138	**Ag** (0.80), **Pb** (0.77), **Zr** (0.65), Hf (0.56), Y (0.53)	Gd, Dy, Ho, Tb (~0.50)	
Aricheng North	U > 500 ppm	988	**Nb** (0.53), Y (0.51)	Sn (0.47), Sc (0.43), La (0.38), Bi (0.38), Ta (0.36), **Ag** (0.34)	SiO$_2$ not analysed. Yb, Ga not analysed. Many Zr analyses of ore samples above UDL of 2000 ppm, thus correlation coefficient (0.18) could be greater.
	All available samples Major Elements	5790	No correlation	No correlation	
	All available samples Minor Elements	5790	**Pb** (0.95)	Bi (0.48), Y (0.42), **Zr** (0.42), **Nb** (0.32)	
Jacque's Lake	U > 500 ppm Minors	793	**Pb** (0.90), **Zr** (0.88), **Ag** (0.71), **Th** (0.67), Hf (0.66), Ge (0.64), REE (0.50–0.65), **Nb** (0.59), Ce (0.53)	Sn (0.50), Y (0.47), Ta (0.42), Yb (0.41)	Few analyses (29) for most REE, Hf, Sn, Ta, Th, Y, Yb & Zr. (Only 6 analyses in high grade samples).
	All available samples Major Elements	29	No correlation	Na$_2$O (0.35)	
	All available samples Minor Elements	4456	**Pb** (0.94), **Th** (0.83), Hf (0.7), Ge (0.67)	**Ag** (0.44), Ga (0.39), V (0.34), REE (~0.35)	

Table 2. *Cont*

Deposit	Sample Population	# Samples	Correlation Coefficients with U >0.50	Correlation Coefficients with U 0.50–0.35	Comments
Rainbow	U > 500 ppm	42	REE (0.96–0.78), **Nb** (0.93), Y (0.93), Sn (0.67), **Th** (0.65), Ta (0.60), Sr (0.54)	Mo (0.50)	Few analyses (17) for most REE, Hf, Sn, Ta, Th, Y, Yb & Zr. Only 8 analyses in high grade samples therefore correlations possibly unreliable.
	All available samples Major Elements	17	CaO (0.57)	No correlation	
	All available samples Minor Elements	353	**Pb** (0.82), Eu (0.81), Hf (0.7), **Ag** (0.69), **Zr** (0.68), Y (0.66), REE (~0.55–0.40)	Mo (0.36)	
Odin	U > 500 ppm	140	**Pb** (0.8)	No correlation	Only 17 elements were analysed for. Suite did not include key elements such as Ag, Be, Nb, REE, Hf, Sn, Y, Ta & Th
	All available samples Major Elements	669	P (0.6)	No correlation	
	All available samples Minor Elements	669	**Pb** (0.84), V (0.56)	**Zr** (0.37) Sr (0.39)	
Duke Batman	U > 500 ppm	4	Na$_2$O (0.86), Al$_2$O$_3$ (56), K$_2$O (0.67), CaO (0.56), Sr (0.97), **Zr** (0.55), **Th** (0.98), Co (0.6), Y (0.56), Ba (0.56), Hf (0.53), REE (>0.45)	**Nb** (0.44), Ta (0.44)	
	All available samples Major Elements	14	No correlation	No correlation	
	All available samples Minor Elements	14	**Th** (0.98), Ni (0.69), Zn (0.62), Y (0.85), Hf (0.63), REE (0.77–0.80, except Nd)	**Nb** (0.41)	Many key elements not analysed for, e.g., Ag, Mo, Se, Be, Ge, *etc*.

6. Discussion

A defining characteristic of this deposit type is the association of uranium ore with albitites, although I note that not all apparently co-genetic uranium deposits in a given district may be hosted by albitite. Albitisation is frequently related to structures of regional and substantial depth extent and is always associated with mylonitisation, cataclasis and brecciation suggesting multiple movements under varying pressure, temperature and depth. It is important to note that albitites are considerably more widespread than uranium deposits they contain and in some instances are associated with IOCG type Cu and Au mineralisation rather than with uranium. A genetic link between albitite uranium and IOCG deposits has yet to be demonstrated.

Another consistent observation is that uranium mineralization post-dates albitisation. This has been attributed to higher intrinsic permeability and porosity of albitised rocks together with superimposed later fracturing [1,2,7,12]. Higher permeabilities and porosities may have been enhanced by dissolution of quartz and K-feldspar, leaving in some cases vuggy cavities. Albitisation probably occurred during ductile deformation (mylonitisation) while uranium seems to have been introduced close to the brittle-ductile transition. Albitisation shows no preference it seems for specific host-rocks, and thus it would appear that the mineralogical nature of the host-rock is irrelevant. Perhaps more significant were

the mechanical properties of albitite relative to the host rocks, that may have contributed to enhanced porosity and permeability.

The presence of substantial volumes of fluorapatite and hydrothermal zircon is a common feature of these deposits. Furthermore, carbonate minerals, particularly Ca- and Mg-rich varieties, are a ubiquitous component of Albitite-type uranium deposits. Bulk Ca abundance can exceed that of Na, tending to invalidate the use of "Na Metasomatite" nomenclature. Bulk chemical analysis generally reveals major loss in SiO_2 and near complete removal of K_2O from host rocks, and good correlation between uranium and a suite of high field strength elements including REE, Nb, Hf and Ta. These elements are seldom present in economic abundance, however, and their mineralogical residence is often poorly documented.

Alteration phases also show a remarkable similarity, with riebeckite, aegirine, garnet, magnetite, hematite, hydrothermal zircon and apatite typically present. Phyllosilicates and epidote tend to be more abundant in the upper parts of zoned orebodies [20]. Presumably higher temperature minerals such as riebeckite, aegirine tend to be present at depth and grade upwards to lower temperature phyllosilicate and/or epidote-rich assemblages.

In most cases, there is no obvious relationship between uranium deposit formation and contemporaneous magmatic intrusions, although the chemical signature of the deposits evokes a carbonatite or possibly alkaline magmatic source. A link to metamorphism has been proposed due to the spatial association of ore deposition with "thermal domes" and generally lower uranium contents of high grade metamorphic rocks, suggesting uranium removal during metamorphism [1]. Clearly, however, further research is needed to confirm or refute the origin of the deposits and their association with metamorphism and magmatism.

Aqueous uranium-sodium-carbonate and phosphate complexes have been proposed to explain transport of uranium into albitite-type deposits [1,16]. The frequent association of uranium with HFSE and dissolution of Si from host-rocks, however, can be rationalised as the product of F-rich gas and/or aqueous fluid [21]. Therefore uranium may have been introduced as a complex with F rather than, or as well as, PO_4 or CO_2. But the nature of the ore-bearing fluids remains poorly defined, partly because quartz is uncommon and fluid inclusions are rare.

Possible depositional mechanisms are likewise ill-defined. Falling temperature has been implicated to explain the change from paragenetically early pyroxene and amphibole at depth to later chlorite and epidote in upperparts of some orebodies [12]. Thus cooling is a potential depositional mechanism, but cooling alone is probably not a satisfactory means of generating ore grade uranium. Another possible depositional mechanism is drop in aqueous CO_2 resulting from the evolution of a CO_2-rich gas phase due to pressure fluctuations, and/or carbonate mineral formation, perhaps as upward moving fluid encountered zones of intense fracturing [1]. Violent phase separation ("boiling") is not likely to be important owing to the lack of indicative mineral textures, and likely formation at substantial depth and therefore confining pressure.

The presence of magnetite and hematite together with anomalous copper in several deposits has led some to infer a genetic link between albitite-type uranium and the IOCG deposit style. There is, however, little evidence of substantial iron addition associated with uranium deposition and albitite-type deposits as a group do not have an affinity for iron-rich host-rocks. Magnetite and hematite in albitite-type uranium deposits may be prograde metamorphic rather than hydrothermal

phases. It is possible that dissolved uranium, in some cases, was precipitated due to reaction with reduced iron, for example, in magnetite. There is no evidence for this, indeed there is a general absence of mineralogical and textural evidence for wall-rock alteration paragenetically related to uranium deposition.

7. Conclusions

Albitite-type uranium deposits account for a substantial portion of the world's potential uranium supply, albeit at relatively low grade. Aspects of the deposits that are reasonably well understood include their structural setting, gangue mineralogy and bulk chemistry. The fine-grained nature of the uranium minerals, however, requires research using tools capable of sub-micron spatial resolution, such as FEG-SEM. Perhaps the biggest unknowns are the nature of the ore-forming fluids and consequently, depositional mechanisms. The ultimate source of the ore-forming fluids is also a key to unlocking the question of whether there is a relationship between albitite-type deposits and carbonatite magmatism or regional metamorphic devolatilisation and focusing along regional fault zones. More data are needed to assess the possibility of a genetic link with IOCG deposits.

Acknowledgments

References

1. Belevtsev, Y.N. Endogenic uranium deposits of precambrian shields: Environment of deposition. In *Albitized Uranium Deposits: Six Articles Translated from Russian Literature*; Abou-Zied, S., Kerns, G., Eds.; U.S. Department of Energy: Washington, DC, USA, 1980; pp. 55–80.
2. Grechishnicov, N.P. Structural setting of one type of uranium-albitite mineralisation in precambrian rocks. In *Albitized Uranium Deposits: Six Articles Translated from Russian Literature*; Abou-Zied, S., Kerns, G., Eds.; U.S. Department of Energy: Washington, DC, USA, 1980.
3. Lobato, L.M.; Fyfe, W.S. Metamorphism, metasomatism, and mineralization at Lagoa Real, Bahia, Brazil. *Econ. Geol.* **1990**, *85*, 968–989.
4. Cordani, U.G.; Iyer, S.S.; Taylor, P.N.; Kawashita, K.; Sato, K.; McReath, I. Pb-Pb, Rb-Sr, and K-Ar systematics of the Lagoa Real uranium province (south-central Bahia, Brazil) and the Espinhao cycle (*ca.* 1.5–1.0 Ga). *J. South Am. Earth Sci.* **1992**, *5*, 33–46.
5. Alexandre, P. Mineralogy and geochemistry of the sodium metasomatism-related uranium occurrence of Aricheng South, Guyana. *Miner Depos.* **2009**, *45*, 351–367.
6. Cinelu, S.; Cuney, M. Sodic metasomatism and U-Zr mineralization: A model based on the Kurupung batholith (Guyana). *Geochim. Cosmochim. Acta* **2006**, *70*, doi:10.1016/j.gca.2006.06.120.
7. Emetz, A.V.; Cuney, M.; Yuzlenko, A.T. Petrochemical Model of Uranium-Mineralized Albitites of the Novokostantynivka Uranium Deposit (Ukraine). In *Proceedings of International Conference on Ore Potential of Alkaline, Kimberlite and Carbonatite Magmatism*, Minsk, Russia, 12–16 September 2011.

8. Maruejol, P.; Cathelineau, M. *Metasomatoses et Mineralisations Uraniferes du Bassin de Krivoi Rog (Ukraine): Le gisement de Zheltorechensk (Mine Novaya)*; CREGU report 87–04; Centre de Recherches sur la Geologie des Matieres Premieres Minerales et Energetiques; Nancy, France, January 1987.

9. Angeiras, A.G. Geology and metallogeny of the northeastern Brazil uranium-phosphorus province emphasizing the Itataia deposit. *Ore Geol. Rev.* **1988**, *3*, 211–225.

10. Netto, A.M.; Meyer, A.; Cuney, M.; Poupou, G. A Thermo-Chronological Study of Itataia Phospho-Uraniferous Deposit (Ceara, Brazil) by Apatite Fission Track Analysis: Genetic Implications. In *Source, Transport and Deposition of Metals*, Proceedings of the 25 Years SGA Anniversary Meeting, Nancy, France, 30 August–3 September 1991; Pagel, M.A., LeRoy, J.L., Eds.; Taylor and Francis Group: Rotterdam, the Netherlands, 1991.

11. Oliver, N.H.; Cleverley, J.S.; Mark, G.; Pollard, P.; Bin, F.; Marshall, L.; Rubenach, M.; Williams, P.; Baker, T. Modeling the role of sodic alteration in the genesis of iron oxide copper-gold deposits, eastern Mount Isa Block, Australia. *Econ. Geol.* **2004**, *99*, 1145–1176.

12. Kalayeav, G.I. Mode of albitite distribution in zones of the ukrainian shield. In *Albitized Uranium Deposits: Six Articles Translated from Russian Literature*; Abou-Zied, S., Kerns, G., Eds.; U.S. Department of Energy: Washington, DC, USA, 1980; pp. 1–13.

13. Beck, L.S. General geology and uranium deposits of the Beaverlodge district. In *Uranium Deposits of Canada*; Evans, E.L., Ed.; Canadian Institute of Mining and Metallurgy: Montréal, Quebec, Canada, 1972; Volume 33, pp. 85–94.

14. Tremblay, L.P. *Geology of the Beaverlodge Mining Area, Saskatchewan*; Department of Energy, Mines and Resources: Ottawa, Canada, 1972.

15. Hoeve, J. *Perspective on Uranium Mineralization at Beaverlodge*; Report G745-1E82 Saskatchewan Research Council: Saskatoon, SK, Canada, 1982.

16. Turek, A. Geology of Lake Cinch Mines Limited, Uranium City, Saskatchewan. Master's Thesis, University of Alberta, Edmonton, Canada, January 1962.

17. Hoeve, J. Uranium metallogenic studies: Relationship between Hudsonian soda metasomatism and Beaverlodge vein-type mineralisation. In *Saskatchewan Geological Survey*; Government of Saskatchewan: Prince Albert, SK, Canada, 1982; pp. 57–59.

18. Ward, D.M. *Uranium Geology of the Beaverlodge Area*; International Atomic Energy Agency: Vienna, Austria, 1984; pp. 269–284.

19. Wilde, A.R.; Otto, A.; Jory, J.; Becker, E.; MacRae, C.; Pownceby, M.; Wilson, N.; Torpy, A. The Valhalla, Bikini & Skal uranium deposits, Mount Isa, Australia. *Miner. Depos.* **2012**, submitted.

20. Olmel'yanenko, B.I.; Mineyeva, I.G. Pre- and syn-ore vertical zonation in Precambrian uraniferous sodic metasomatites. *Int. Geol. Rev.* **1982**, *24*, 422–430.

21. Netto, A.M. Contributions a la Mineralogie a la Petrographie et a la Metallogenie du gisement Phospho-Uranifere D'Itataia, Ceara, Bresil. Ph.D. Thesis, Université de Clermont-Ferrand, Clermont-Ferrand, France, 1984.